Bioorganic & Medicinal Chemistry Letters 20 (2010) 6291–6296

Contents lists available at ScienceDirect

Bioorganic & Medicinal Chemistry Letters

journal homepage: www.elsevier.com/locate/bmcl

Piperidine-based renin inhibitors: Upper chain optimization

Olivier Corminboeuf, Olivier Bezençon *, Ľuboš Remeň, Corinna Grisostomi, Sylvia Richard-Bildstein, Daniel Bur, Lars Prade, Panja Strickner, Patrick Hess, Walter Fischli, Beat Steiner, Alexander Treiber

Drug Discovery Chemistry & Biochemistry, Actelion Pharmaceuticals Ltd, Gewerbestrasse 16, 4123 Allschwil, Switzerland

ARTICLE INFO

Article history:
Received 15 June 2010
Revised 17 August 2010
Accepted 17 August 2010
Available online 22 August 2010

Keywords:
Hypertension
Renin angiotensin aldosterone system
Renin inhibitor
Piperidine

ABSTRACT

The optimization of the 4-position of recently described new 3,4-disubstituted piperidine-based renin inhibitors is reported herein. The synthesis and characterization of compounds leading to the discovery of **11** (**ACT-178882**, **MK-1597**), a renin inhibitor with a suitable profile for development is described.

In the preceding article,[1] starting from diazabicyclononenes of type **1** and tetrahydropyridines of type **2** (Fig. 1), we reported new piperidine derivatives with an optimized amide side chain attached at the 3-position of the piperidine ring. This work culminated in the discovery of piperidines **3** and **4** (Fig. 1), two renin inhibitors with excellent efficacies when administered at low dose to double transgenic rats harboring both the human angiotensinogen and the human renin gene.[2] Unfortunately, both compounds suffered from unfavorable CYPs interactions.[1]

Extensive studies on the *meta*-position of the benzyl amide residue R2 had shown that the CYP3A4 interactions could be modulated by introduction of hydrophilic groups, but, at the price of a reduced potency in human plasma. We also showed that the introduction of a hydroxyl group at the 4-position of the piperidine was tolerated regarding activity on the target but did not bring further benefits on CYP3A4 inhibition. We report here our efforts to further improve the profile of this series by new modifications of the 4-substituent of the central piperidine.

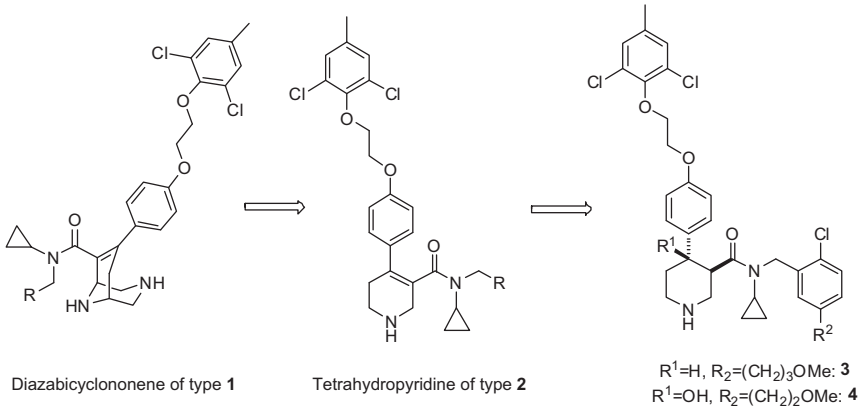

Figure 1. Design leading to 3,4-disubstituted piperidines 3 and **4** from diazabicyclononenes of type **1** and tetrahydropyridines of type **2**.

* Corresponding author. Tel.: +41 61 565 65 77; fax: +41 61 565 65 00.
E-mail address: olivier.bezencon@actelion.com (O. Bezençon).

0960-894X/$ - see front matter © 2010 Elsevier Ltd. All rights reserved.
doi:10.1016/j.bmcl.2010.08.087

Inspired by the work of Güller et al.[3] the phenyl ring at the 4-position of the piperidine was first replaced by a pyridyl. Acid **9** was accessed starting from the known alcohol **5**,[4] displacing first the 2-bromo substituent of 2,5-dibromopyridine **6**, followed by a Negishi coupling with the known triflate **7** (Scheme 1). Magnesium-based reduction[5] of the double bond, followed by isomerization to the thermodynamically favored *trans* ester and saponification afforded the desired acid **9**. Final compounds **10**–**21** were obtained by coupling of the corresponding acid with a set of amines followed by deprotection and separation of the enantiomers by HPLC using a chiral stationary phase (Regis R,R Whelk 01 column).

Table 1 shows comparisons between the new derivatives comprising a pyridyl moiety at the piperidine 4-position (Y = N) and the phenyl analogues reported earlier (Y = CH).[1] The introduction of the pyridyl moiety allowed to reach sub-nanomolar potencies in plasma (entries 5 and 13) but had only a minor effect on the CYP3A4 competitive inhibition and even tended to increase the time-dependent inhibition after 30 min of pre-incubation in the presence of liver microsomes (TDI_{30}). Derivative **10** is a relevant exception since the TDI_{30} is reduced by a factor >3 (entry 2 vs 1), yielding along with derivatives **11** and **15** the compounds with the lower shift.

Encouraged by those results (reduction of the buffer to plasma shift and CYP3A4 parameters such as for compounds **10** and **11**), we introduced further modifications at the piperidine 4-position, focusing on the introduction of residues with slightly increased hydrophilic properties. The aryl–aryl linker had been shown to tolerate introduction of five-membered heterocycles at different positions in the diazabicyclononene series (unpublished results). An isoxazole such as the one described in compounds **27**–**31** had proven to be the most suitable replacement (Scheme 2). To access acid **26**, a new synthetic pathway had to be designed due to the intrinsic reactivity of the isoxazole moiety: to avoid side-reaction, the double bond at the 3,4-positions of the piperidinyl ring had to be reduced before the introduction of the isoxazole. Therefore, benzyl-protected bromophenol was coupled with triflate **7** under the Negishi conditions reported previously. Reduction of the double bond followed by isomerization afforded the more stable *trans* product. Palladium-catalyzed benzyl deprotection delivered phenol **23** which could be coupled under Mitsunobu conditions with alcohol **25**. This compound **25** was obtained by 2,3-dipolar cycloaddition of propargylalcohol with the nitrile oxide resulting from treatment of aldehyde **24** with hydroxylamine followed by oxidation. Saponification of the ester resulting from the Mitsunobu coupling afforded acid **26**. Standard amide coupling with a set of

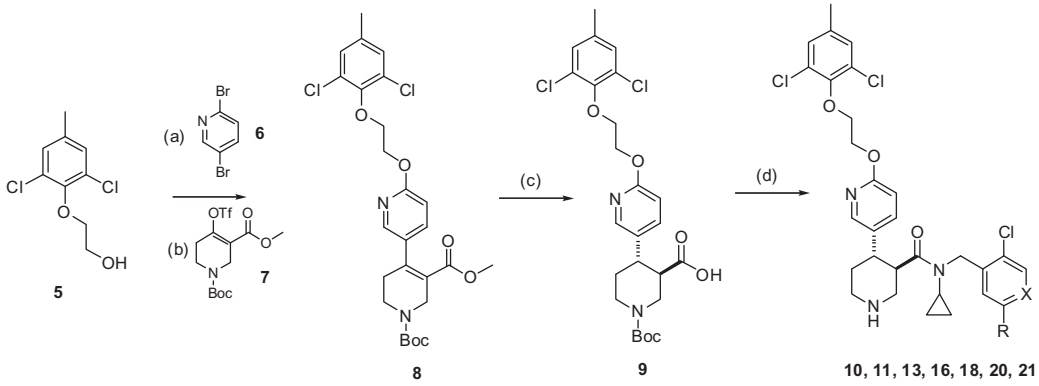

Scheme 1. Synthetic pathway leading to 3-amido-4-pyridyl piperidines. Reagents and conditions: (a) (i) 1.25 equiv NaH, THF, 0 °C, 1 h; (ii) 1.05 equiv **6**, THF, reflux, 2 h, 75%; (b) (i) 1.5 equiv *n*-BuLi, THF, −78 °C; (ii) 1.68 equiv ZnCl2 1 M in THF, −78 °C to rt; (iii) 1.0 equiv **7**, 0.03 equiv $Pd(PPh_3)_4$, THF, rt, 16 h, 62%; (c) (i) 1.2 equiv Mg, MeOH, rt, 2 h, 78%; (ii) MeONa, MeOH, 70 °C, 3 h, 75%; (d) (i) 1.25 equiv HOBt, 4.0 equiv DIPEA, 0.25 equiv DMAP, 1.5 equiv amine; (ii) HCl 4 N in dioxane, CH_2Cl_2, 1.5 h, 0 °C; (iii) Chiral HPLC (Regis R,R Whelk 01 column).

Table 1
4-Pyridine introduction: in vitro characterization

	Entry	Compd	Y	X	R	Renin IC_{50} (nM)		Buffer to plasma shift	CYP3A4 (μM)		CYP3A4 TDI_{30}
						Buffer	Plasma		Mid	Test	
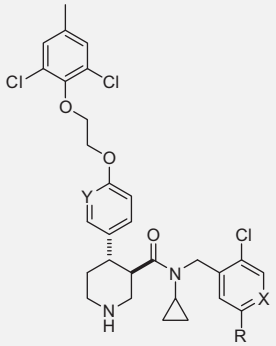	1	**3**	CH	CH	$-(CH_2)_3OMe$	0.33	11.8	36	4.8	8.1	18
	2	**10**	N	CH	$-(CH_2)_3OMe$	0.16	3.6	23	3.3	-	5
	3	**11**	N	CH	$-(CH_2)_2OMe$	0.07	1.4	20	3.3	4.5	6.8
	4	**12**	CH	CH	$-(CH_2)_2NHAc$	0.18	1.4	8	2.4	6	8.7
	5	**13**	N	CH	$-(CH_2)_2NHAc$	0.08	0.9	11	1.9	6.7	15
	6	**14**	CH	CH	$-(CH_2)_2OMe$	0.18	8.1	45	3.2		
	7	**15**	CH	CH	$-CH_2NHC(O)CH_2CF_3$	0.27	6.9	26	4	7.9	4.5
	8	**16**	N	CH	$-CH_2NHC(O)CH_2CF_3$	0.17	2.6	51	3.0	8.4	16
	9	**17**	CH	CH	$-CH_2NHC(O)OMe$	0.09	2.0	22	3.5	6.5	12
	10	**18**	N	CH	$-CH_2NHC(O)OMe$	0.05	2.1	42	2.5	3.5	18
	11	**19**	CH	N	$-(CH_2)_3OMe$	0.28	3.5	13	5.9		13
	12	**20**	N	N	$-(CH_2)_3OMe$	0.14	1.9	14	2.1		15
	13	**21**	N	NO	$-(CH_2)_3OMe$	0.08	0.5	6	1.6	4.4	12

3, 10-21

Mid: midazolam as a marker. Test: testosterone as a marker. The CYP3A4 TDI_{30} value represents the ratio of the CYP3A4 IC_{50} at t_0 to the CYP3A4 IC_{50} after 30 min of pre-incubation in the presence of liver microsomes.

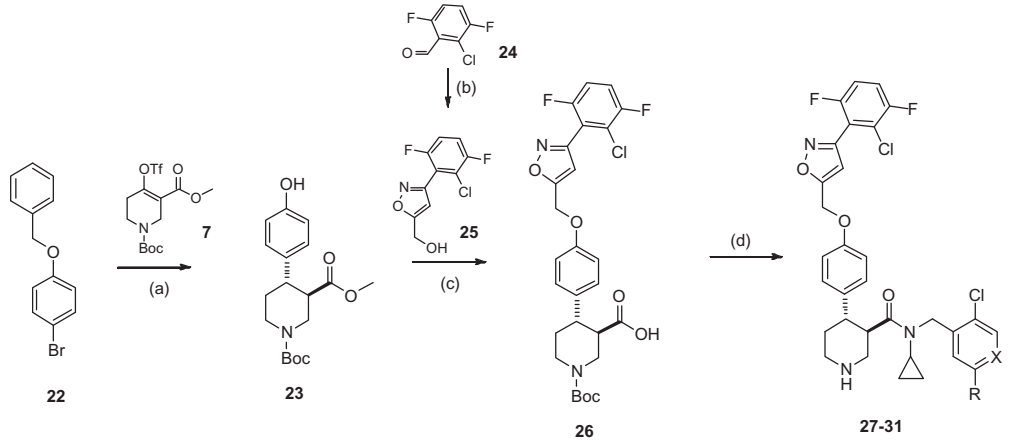

Scheme 2. Synthetic pathway leading to isoxazole containing linker. Reagents and conditions: (a) (i) 1.0 equiv *n*-BuLi, THF, −78 °C, 30 min; (ii) 1.2 equiv $ZnCl_2$ 1 M in THF, −78 °C to rt; (iii) 0.7 equiv **7**, 0.02 equiv $Pd(PPh_3)_4$, THF, 50 °C, 1 h, 86%; (iv) 3.0 equiv Mg, MeOH, rt, 2 h, 85%; (v) MeONa, MeOH, 70 °C, 6 h, 89%; (vi) 10% $Pd(OH)_2$, H_2, MeOH, 16 h, 99%; (b) (i) 2.0 equiv hydroxylamine hydrochloride, 3.0 equiv $NaHCO_3$, 0.05 equiv tetrabutylammonium chloride, water/acetonitrile 2/1, rt, 1 h, 96%; (ii) 0.8 equiv propargylalcohol, 1.0 equiv Et_3N, 1.0 equiv *N*-chlorosuccinimide, DMF, 85 °C, 1 h, 72%; (c) (i) 1.0 equiv **23**, 1.3 equiv **25**, 2.0 equiv 1,1′-(azodicarbonyl)dipiperidine, 4.0 equiv PBu_3, toluene, 80 °C, 1 h, 90%; (ii) 8 equiv NaOH 1 M, THF, 70 °C, 16 h, 77%; (d) (i) 1.25 equiv HOBt, 4.0 equiv DIPEA, 0.25 equiv DMAP, 1.5 equiv amine; (ii) HCl 4 N in dioxane, CH_2Cl_2, 1.5 h, 0 °C; (iii) Chiral HPLC (Regis R,R Whelk 01 column).

Table 2
Isoxazole introduction: in vitro characterization

Entry	Compd	X	R	Renin IC_{50} (nM)		Buffer to plasma shift	CYP3A4 (μM)		CYP3A4 TDI_{30}
				Buffer	Plasma		Mid	Test	
1	**27**	CH	$-(CH_2)_2NHAc$	0.09	0.5	6	1.7	3.7	2.4
2	**28**	CH	$-(CH_2)_3OMe$	0.17	6.6	39	1.8		25
3	**29**	CH	$-CH_2NHC(O)OMe$	0.15	0.9	6	1.1	2.2	7.5
4	**30**	N	$-(CH_2)_3OMe$	0.17	0.5	3	1.9	3.6	11
5	**31**	NO	$-(CH_2)_3OMe$	0.12	0.3	3	1.8	4.1	

Mid: midazolam as a marker. Test: testosterone as a marker. The CYP3A4 TDI_{30} value represents the ratio of the CYP3A4 IC_{50} at t_0 to the CYP3A4 IC_{50} after 30 min of pre-incubation in the presence of liver microsomes.

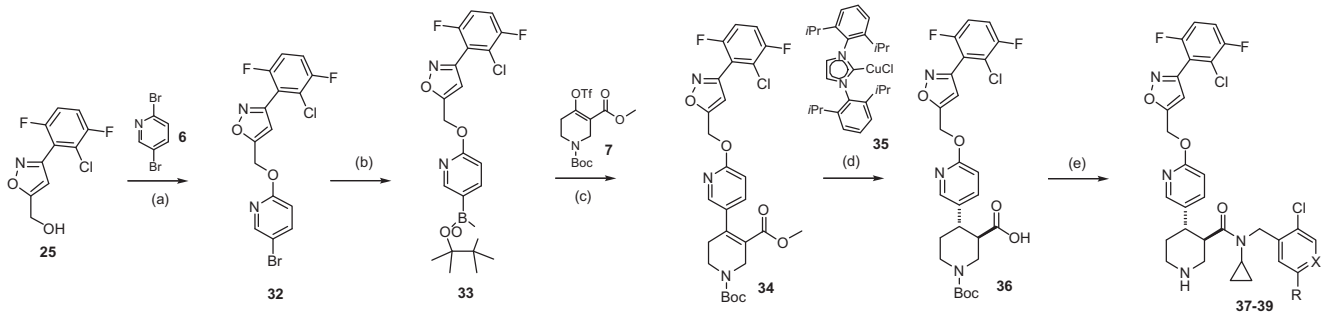

Scheme 3. Synthetic pathway leading to pyridine-isoxazole linker. Reagents and conditions: (a) 1.3 equiv **6**, 1.5 equiv *t*BuONa, 0.06 equiv 4.5-bis(diphenylphosphino)-9,9-dimethylxanthene, 0.02 equiv $Pd(PPh_3)_4$, toluene, 110 °C, 1 h, 43%; (b) 1.5 equiv 4,4,5,5-tetramethyl-1,3,2-dioxaborolane, 3.0 equiv Et_3N, 0.03 equiv $Pd_2Cl_2(PPh_3)_2$, dioxane, 100 °C, 16 h, 78%; (c) 0.75 equiv **7**, 9 equiv Na_2CO_3 2 M, 0.04 equiv $Pd(PPh_3)_4$, DME, 80 °C, 1 h, 40%; (d) (i) 0.1 equiv **35**, 0.1 equiv *t*BuONa, 12 equiv poly(methylhydrosiloxane, *t*BuOH, rt, 3 h, 86%; (ii) 1.5 equiv MeONa, MeOH, 70 °C, 16 h, 40%; (iii) 10 equiv NaOH 1 M, MeOH, 90 °C, 1 h, 98%; (e) (i) 1.25 equiv HOBt, 4.0 equiv DIPEA, 0.25 equiv DMAP, 1.5 equiv amine; (ii) HCl 4 N in dioxane, CH_2Cl_2, 0 °C, 1 h; (iii) Chiral HPLC (Regis R,R Whelk 01 column).

Table 3
Pyridine/oxazole combination: in vitro characterization

Entry	Compd	X	R	Renin IC_{50} (nM)		Buffer to plasma shift	CYP3A4 (μM)		CYP3A4 TDI_{30}
				Buffer	Plasma		Mid	Test	
1	**37**	CH	$-(CH_2)_2OMe$	0.05	0.6	12		1.1	8.5
2	**38**	N	$-(CH_2)_3OMe$	0.13	0.5	4		3.3	14.7
3	**39**	NO	$-(CH_2)_3OMe$	0.20	0.2	1		5.1	1.8

Mid: midazolam as a marker. Test: testosterone as a marker. The CYP3A4 TDI_{30} value represents the ratio of the CYP3A4 IC_{50} at t_0 to the CYP3A4 IC_{50} after 30 min of pre-incubation in the presence of liver microsomes.

selected amines followed by deprotection and separation of the enantiomers by HPLC using a chiral stationary phase (Regis R,R Whelk 01 column) allowed to access the desired products.

In general, the introduction of the isoxazole moiety had a more pronounced effect than the pyridine on the reduction of the buffer to plasma shift (compare Table 2, entries 1, 3–5 with Table 1, entries 2, 10, 12, and 13, respectively). Most compounds had sub-nanomolar potencies toward renin, even in presence of 100% human plasma (Table 2), bringing those compounds at the level of plasma potency of aliskiren (IC_{50} = 0.6 nM in human plasma).[6] However, the isoxazole moiety did not prevent the CYP3A4 competitive inhibition and the TDI_{30}.

Positive effects on CYP3A4 time-dependent inhibition have been observed in the case of the isoxazole derivatives and a reduced buffer to plasma shift was observed for both the pyridine and isoxazole derivatives. In order to determine if the combination of both these elements would have synergistic effects, the synthesis of acid **36** was undertaken (Scheme 3). In a first synthetic approach, it was not possible to reduce the tetrahydropyridyl double bond efficiently before introducing the isoxazole, presumably due to the presence of the pyridine ring. We therefore decided to carry out the reduction on the whole template already containing the isoxazole. To do so, a different methodology had to be applied to allow for the reduction of the double bond without reducing the isoxazole moiety of compound **34**.

The synthetic pathway described in Scheme 3 takes advantage of the availability of alcohol **25** which was coupled with 2,5-dibromopyridine under palladium based catalysis. Since the resulting bromide **32** was not suitable to undergo the Br/Li exchange used so far for the Negishi coupling, we had to use a Suzuki coupling. The boronic ester **33** was prepared by palladium-catalyzed exchange and used directly in the Suzuki coupling. The magnesium reduction methodology was first tried to reduce the double bond but over-reduction and cleavage of the side chain were observed. Using L-selectride®,[7] reduction of the ester to the corresponding alcohol occurred while the use of sodium borohydride in the presence of cobalt(II) dichloride[8] led to selective and clean reduction of the isoxazole. Only a copper catalyzed reduction developed by the groups of Buchwald and Sadighi[9] led to a clean and efficient reduction of the double bond. Further equilibration to the *trans* compound followed by saponification of the ester afforded the desired acid **36**. Due to the challenges encountered during the synthesis of this building block, it was only coupled with a small selection of amines.

Table 3 shows that combining the pyridine and the oxazole moieties still yielded compounds with sub-nanomolar plasma activities. Unfortunately, and despite the introduction of these two heteroaromatic rings, except for compound **39**, CYP3A4 inhibition and TDI_{30} were still unsatisfactory. We did not further pursue this route and turned to a combination of a pyridine moiety and a pyrrolidinol.

Synthetic access to this class of compounds was straightforward starting from enantiomerically pure pyrrolidinol **40**. After nucleophilic substitution on 2,5-dibromopyridine, the resulting alcohol was coupled with phenol **41** under Mitsunobu conditions to deliver bromide **42** (Scheme 4). Further coupling under Negishi conditions with the triflate **7** followed by magnesium-based double bond reduction and equilibration under basic conditions afforded the thermodynamically favored *trans* ester. Saponification afforded acid **43**. Standard amide coupling with a set of selected amines followed by deprotection and separation of the enantiomers by HPLC using a chiral stationary phase (Regis R,R Whelk 01 column) allowed to access the desired products.

Both the *R*- and the *S*-pyrrolidine derivatives were prepared and were shown to lead to equipotent inhibitors. In comparison with the previously described classes, a higher buffer to plasma shift

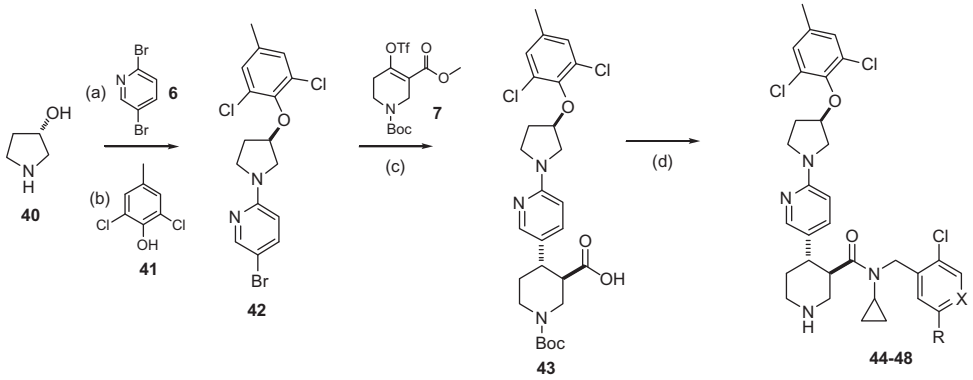

Scheme 4. Synthetic pathway leading to pyrrolidino-pyridine derivatives. Reagents and conditions: (a) 1.05 equiv 2,5-dibromopyridine, 1.2 equiv DIPEA, toluene, 110 °C, 22 h, 44%; (b) 1.1 equiv 2,6-dichloro-*p*-cresol, 1.25 equiv azodicarboxylic dipiperidide, 1.5 equiv PPh_3, toluene, 100 °C, 2 h, 93%; (c) (i) 1.5 equiv *n*-BuLi, THF, −78 °C, 30 min; (ii) 1.8 equiv $ZnCl_2$ 1 M in THF, −78 °C to rt; (iii) 1.0 equiv **7**, 0.05 equiv $Pd(PPh_3)_4$, THF, 65 °C, 1 h, 43%; (iv) 5.0 equiv Mg, MeOH, rt, 2 h; (v) MeONa, MeOH, 70 °C, 16 h, 58%; (vi) 8 equiv NaOH 1 M, THF, 70 °C, 6 h, 98%; (d) (i) 1.25 equiv HOBt, 4.0 equiv DIPEA, 0.25 equiv DMAP, 1.5 equiv amine; (ii) HCl 4 N in dioxane, CH_2Cl_2, 1.5 h, 0 °C; (iii) Chiral HPLC (Regis R,R Whelk 01 column).

Table 4
Pyrrolidino-pyridine derivative: in vitro characterization (*R* and *S* refer the pyrroline chirality)

Entry	Compd	X	R	Renin IC_{50} (nM)		Buffer to plasma shift	CYP3A4 (μM)		CYP3A4 TDI_{30}
				Buffer	Plasma		Mid	Test	
1	*R*-**44**	CH	$-(CH_2)_2OMe$	0.12	3.9	33	14	3.2	1.4
2	*S*-**45**	CH	$-(CH_2)_2OMe$	0.44	5.0	11	1.0	2.5	1.5
3	*R*-**46**	N	$-(CH_2)_3OMe$	0.21	1.8	9	3.5	8.4	1
4	*R*-**47**	NO	$-(CH_2)_3OMe$	0.10	0.7	7	1.2	2.9	1.9
5	*S*-**48**	NO	$-(CH_2)_3OMe$	0.1	1.0	10	0.7	2.4	7.3

Mid: midazolam as a marker. Test: testosterone as a marker. The CYP3A4 TDI_{30} value represents the ratio of the CYP3A4 IC_{50} at t_0 to the CYP3A4 IC_{50} after 30 min of pre-incubation in the presence of liver microsomes.

Table 5
4-Hydroxy introduction effect on in vitro compound profile

	4	**53**	**54**	**55**
Ar	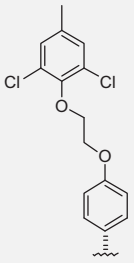	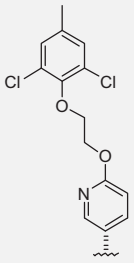	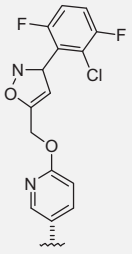	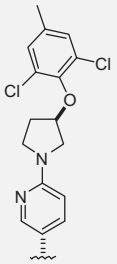
IC_{50} buffer	0.24 nM	0.12 nM	0.20 nM	0.15 nM
IC_{50} plasma	5.6 nM	3.8 nM	0.5 nM	1.2 nM
shift	23	32	2.5	8
$CYP3A4_{mid}$	1.4 μM	1.2 μM	–	0.6 μM
$CYP3A4_{test}$	4.6 μM	2.9 μM	0.8 μM	2 μM
CYP3A4 TDI	2.4	3.2	3.5	–

Mid: midazolam as a marker. Test: testosterone as a marker. The CYP3A4 TDI_{30} value represents the ratio of the CYP3A4 IC_{50} at t_0 to the CYP3A4 IC_{50} after 30 min of pre-incubation in the presence of liver microsomes.

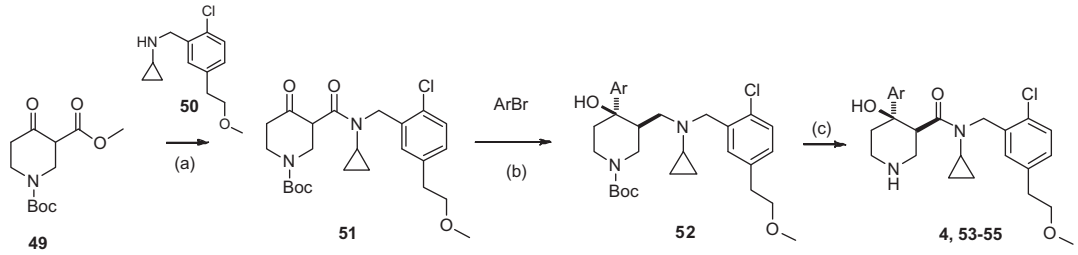

Scheme 5. Reagents and conditions: (a) 1.1 equiv amine **50**, 0.13 equiv *p*-TsOH, toluene, 110 °C, 16 h, 75–85%; (b) (i) 2.5 equiv ArBr, THF, 2.75 equiv *n*-BuLi, −78 °C, 30 min; (ii) 5.5 equiv DMPU, amide, THF, −78 °C, 10 min; (c) (i) 15 equiv HCl 4 M in dioxane, CH_2Cl_2, 0 °C, 1 h, 60–75%; (ii) Chiral HPLC (Regis R,R Whelk 01 column).

Table 6
In vivo characterization of modified piperidine-based renin inhibitors at a dose of 3 mg/kg po

	Compd	$IC_{50Plasma}$ (nM)	ABC	Max	$T_{1/2}$	Cl	%*F*
1	**15**	6.9	−304	−19	–	–	–
2	*S*-**46**	1.8	−141	−9	–	–	–
3	**39**	0.2	−134	−12	–	–	–
4	*R*-**44**	3.9	−1633	−37	5.6	35	8
5	**11**	1.4	−2380	−50	5.8	21	35
6	**10**	4.0	−2219	−45	3.6	29	28

Activity in plasma as EC_{50} in nM, Max stand for maximal blood pressure reduction in mmHg, $T_{1/2}$ in hour, Cl in mL/min kg. ABC stands for area between the curves (mmHg h), MAP stands for mean arterial pressure (mmHg).

was observed. Interestingly, compounds with a higher shift had a more suitable CYP3A4 profile while compounds with the lower shifts suffered from CYP3A4 inhibition issues.

We then decided to remove the double bond and to introduce a hydroxy substituent at the 4-position as reported previously for 4-hydroxypiperidine **4**[1] (Table 5). Applying a convergent synthesis and using preferred amine **50**, chosen based on synthetic accessibility and previous results, the targeted compounds could be obtained in a short and efficient way (Scheme 5).

The introduction of the hydroxy group at the 4-position significantly improved the time-dependent CYP3A4 inhibition but did not solve the CYP3A4 competitive inhibition (Table 5).

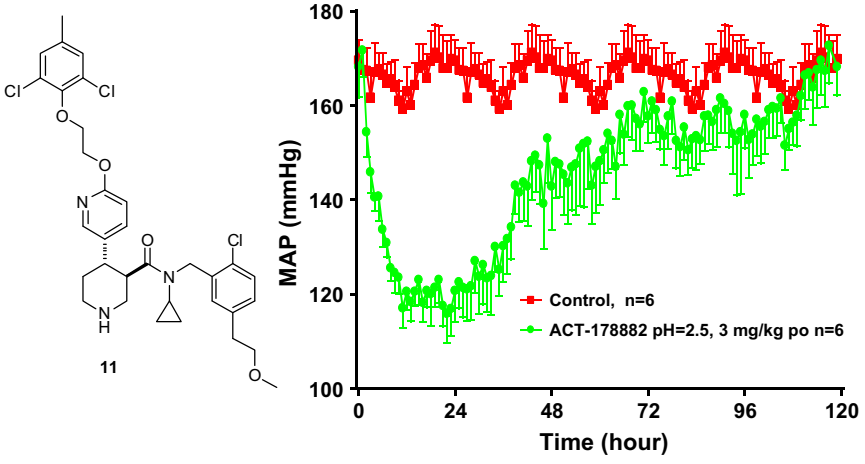

Figure 2. Pharmacodynamic behavior of ACT-178882/MK1597.

Based on the overall profile of the compounds, six of them were chosen for pharmacodynamic characterization by administration to double transgenic rats harboring both the human angiotensinogen and the human renin gene[2] (Table 6). Three compounds (**15**, *S*-**46** and **39**) displayed insufficient in vivo efficacy (Table 6, entries 1–3) and were dropped. The three remaining compounds showed a suitable efficacy profile and were further characterized. Despite an unsatisfactory low bioavailability (8%), pyrrolidine *R*-**44** (Table 4, entry 1) showed a surprisingly high efficacy. Piperidines **10** and **11** showed a suitable PK profile for further development. Based on a higher potency toward renin in human plasma, **11** (**ACT-178882**/**MK-1597**, Fig. 2) was selected for further development.

In conclusion, we modified the 4-substituent of a new series of piperidine-based renin inhibitors and explored the properties of the compounds by inserting small hydrophilic modifications. This work culminated in the discovery of **11** (**ACT-178882**/**MK-1597**), a new renin inhibitor with a suitable profile for further development.

References and notes

1. Corminboeuf, O.; Bezençon, O.; Remeň, Ľ.; Grisostomi, C.; Richard-Bildstein, S.; Bur, D.; Prade, L.; Strickner, P.; Hess, P.; Fischli, W.; Steiner, B.; Treiber, A. *Bioorg. Med. Chem. Lett.*, **2010**, *20*, 6286.
2. (a) Brockway, B. P.; Mills, P. A.; Azar, S. H. *Clin. Exp. Hyper.—Theory Pract.* **1991**, *13*, 885; (b) Guiol, C.; Ledoussal, C.; Surgé, J.-M. *J. Pharmcol. Toxicol. Methods* **1992**, *28*, 99; (c) Hess, P.; Clozel, M.; Clozel, J.-P. *J. Appl. Physiol.* **1996**, *81*, 1027.
3. Güller, R.; Binggeli, A.; Breu, V.; Bur, D.; Fischli, W.; Hirth, G.; Jenny, C.; Kansy, M.; Montavon, F.; Müller, M.; Oefner, C.; Stadler, H.; Vieira, E.; Wilhelm, M.; Wostl, W.; Märki, H. P. *Bioorg. Med. Chem. Lett.* **1999**, *9*, 1403.
4. Bezençon, O.; Bur, D.; Weller, T.; Richard-Bildstein, S.; Remeň, Ľ.; Sifferlen, T.; Corminboeuf, O.; Grisostomi, C.; Boss, C.; Prade, L.; Delahaye, S.; Treiber, A.; Strickner, P.; Binkert, C.; Hess, P.; Steiner, B.; Fischli, W. *J. Med. Chem.* **2009**, *52*, 3689.
5. Meltzer, P. C.; Blundell, P.; Yong, Y. F.; Chen, Z.; George, C.; Gonzalez, M. D.; Madras, B. K. *J. Med. Chem.* **2000**, *43*, 2982.
6. Rahuel, J.; Rasetti, V.; Maibaum, J.; Rüeger, H.; Göschke, R.; Cohen, N.-C.; Stutz, S.; Cumin, F.; Fuhrer, W.; Wood, J. M.; Grütter, M. G. *Chem. Biol.* **2000**, *7*, 493.
7. Fortunato, J. M.; Ganem, B. *J. Org. Chem.* **1976**, *41*, 2194.
8. Ihara, M.; Tokunaga, Y.; Fukumoto, K. *J. Org. Chem.* **1990**, *55*, 4497.
9. Jurkauskas, V.; Sadighi, J. P.; Buchwald, S. *Org. Lett.* **2003**, *5*, 2417.